



## Synthesis of nanostructured hydroxyapatite in presence of polyethylene glycol 1000

K. Azzaoui<sup>1</sup>, A. Lamhamdi<sup>1</sup>, E. Mejdoubi<sup>1</sup>, M. Berrabah<sup>1</sup>, A. ELidrissi<sup>2</sup>, B. Hammouti<sup>2</sup>, S. Zaoui<sup>1</sup> and R. Yahyaoui<sup>1</sup>

<sup>1</sup>L.C.S.M.A. Faculté des Sciences, Université Mohammed I, Oujda, Morocco  
<sup>2</sup>LCAE-URAC18. Faculté des Sciences, Université Mohammed I, Oujda, Morocco

### ABSTRACT

Composite materials have showing potential applications in biomaterials. Among the composite materials, HAp/polymer possesses significant advantages of high mechanical reliability and excellent biocompatibility for applications involving artificial bones and teeth. The aim of this study was to develop nanocomposites of hydroxyapatite and polyéthylène glycol (HAp/ PEG 1000), also the study of the adsorption of the bisphenol A (PBA) with composite synthesized. The structure were synthesized and characterized by X-ray diffraction (XRD), Fourier transform infrared spectroscopy (FTIR), and field emission-scanning electron microscopy (FE-SEM). The results revealed that the size of HAp nanoparticles decrease with increase in PEG concentration in the composite. SEM image shows particles with an average diameter of 50 to 60 nm. Furthermore, At elevated temperatures the molecules of polyethylene glycol is evaporated and leads to the formation of platelet HAP.

**Key words:** Hydroxyapatite, composite Biomaterials, Poly ethylene glycol, Adsorption, GC/MS/SIM.

### INTRODUCTION

Hydroxyapatite (HAp) is the most applied calcium phosphate as bone substitutes because of its chemical similarity to the natural calcium phosphate mineral present in biological hard tissues. Different clinical applications involve repair of bone defects, bone augmentation, as well as coatings for metallic implants [1]. The important condition of a material designed for bone substitution a, is the ability to create a bond with the host living bone [2]. Therefore, researchers have tried to customize its properties such as bioactivity, mechanical strength and solubility by controlling its composition, morphology and particle size [3, 4]. The morphological and chemical properties of synthetic hydroxyapatite can be modulated by varying the method and conditions of synthesis. There are several different methods used to synthesize HAP as reported in the literature including chemical precipitation [1], hydrothermal techniques [5], sol-gel, solid state and mechano- chemical methods [6, 7]. Recently much attention have been made to develop nanocrystalline structure with controlled morphology [8-11], several organic modifiers are used such as ethylene glycol [9], cetyltrimethylammonium bromide (CTAB) [8, 12], polyvinyl alcohol [12], citric acid [13] and ethylenediaminetetraacetic acid (EDTA), [14].

The present work describe synthesis of nanostructured hydroxyapatite by method using calcium nitrate tetra hydrate and di-ammonium hydrogen phosphate as starting materials, using polyethylene glycol (MW 1000) as modifier. The explanation about the effect of the polyethylene glycol for synthesis of hydroxyapatite with controled size is attempted.

## EXPERIMENTAL SECTION

### 2.1. Materials and methods

Polyethylene glycol (MW 1000),  $\text{Ca}(\text{NO}_3)_2 \cdot 4\text{H}_2\text{O}$  (99 %),  $(\text{NH}_4)_2\text{HPO}_4$  (99 %) and ammonia, were purchased from Aldrich. High purity distilled water was used throughout the whole experiment.

The starting materials used in the synthesis of hydroxyapatite were analytical grade reagents, the calcium nitrate tetra hydrate and di-ammonium hydrogen phosphate. HAp was synthesized by following a modified wet chemical method. At 25 °C, 11.76 g of  $\text{Ca}(\text{NO}_3)_2 \cdot 4\text{H}_2\text{O}$  was first dissolved in a 100 ml volume of water. A solution of 4.06 g  $(\text{NH}_4)_2\text{HPO}_4$  was dissolved in 100 ml volume of water and then added to the  $\text{Ca}(\text{NO}_3)_2 \cdot 4\text{H}_2\text{O}$  solution over a period of 30 min. The amount of reagents in the solution was calculated to obtain a Ca/P molar ratio value equals 1.67, corresponding to a stoichiometric HAp. The polyethylene glycol was added along with the mixture. The pH of the slurry was measured digitally during the precipitation reaction, reaching a final value of pH 10.5 (Fig. 1).

### 2.2. Preparation of standards and sample solution

The standard stock solution was prepared by accurately weighting 100 mg of BPA into 1L ( $S_0$ ) volumetric flask and dissolved in distilled water. The stock solution was diluted with distilled water to obtain solutions  $S_1$  and  $S_2$ , 10 and 1 mg/L, respectively.

Prior to use thin powders were washed with the deionised water, absolute ethanol and dried in the oven at 120 °C for 1hour in order to remove impurities and any possible residual analytes (interferences). Extraction and desorption were carried out as follows: thin powders were immersed in 50 mL of  $S_2$  in a glass vial under stirring (contact 20 min), after extraction, the thin powders were filtered and dried with a filter paper and put in an oven to dry at 40 °C for 40 min. finally, the thin powders were directly placed in centrifuge tube (1.5 ml) to desorb and derive target analyte BPA with BSTFA 1% TMCS (200  $\mu\text{L}$ ) under sonication and heated at 70 °C for 30 min. Of the final 0.2 mL final derivative solution, 1  $\mu\text{L}$  was directly injected into the Shimadzu GC/MS system for analysis. In each experiment, the analyte concentration was the same and each solution were analysed in triplicate.

### 3.4. Conditions of BPA analysis

GC/MS system: A Shimadzu GCMS-QP2010 (Shimadzu, Japan) with GCMS solution 2.5 software. **Chromatographic conditions:** GC analysis was performed on a Shimadzu QP 2010 system with a fused silica capillary column (30 m, 0.25mm i.d. and film thickness of 0.25 mm with chemically bonded phase DB-5). The oven temperature was held at 60 °C for 1 min and programmed to rise at 10 °C  $\text{min}^{-1}$  to 280 °C and held for 5 min. A sample volume of 0.1–1  $\mu\text{L}$  was injected in splitless mode (high pressure). The injector and interface temperature was kept at 250 °C. Helium was used as the carrier gas.

**Spectrometric conditions:** Mass spectrometric parameters: the electron impact ionization energy was 70 eV, the detector voltage 1.7 kV, the ion source temperature was 200°C and the solvent delay time was 3 min. MS detector was used in multiple ion monitoring mode (ions characteristic of BPA in SIM mode were :  $m/z = 357$  and  $372$ ) [15].

### 4.5. Physical-chemical characterization

The prepared samples were studied by Fourier transform infrared spectroscopy (FTIR) using a Shimadzu FT-IR 300. The FTIR spectra were obtained over the region 400 to 4000  $\text{cm}^{-1}$  in pellet form for 1 mg powder samples mixed with 200 mg spectroscopic grade (KBr). The structure of the samples were analyzed by X-ray diffraction (XRD) using a diffractometer system =XPERT-PRO with Cu-K $\alpha$ 1 radiation ( $\lambda = 1.5418 \text{ \AA}$ ). This peak assigns to (002) Miller's plane family and shows the crystal growth along the axis of HAp crystalline structure. The morphology of the materials was analyzed by field emission-scanning electron microscopy (SEM). GC/MS system: A Shimadzu GCMS-QP2010 (Shimadzu, Japan) with GCMS solution 2.5 software.

## RESULTS AND DISCUSSION

### 3.1 Chemical structure

#### 3.1.1. XRD analysis

The XRD patterns of hydroxyapatite and hydroxyapatite using polyethylene glycol as modifier. The patterns indicate the presence of well crystallized hydroxyapatite. The X-ray patterns collected on the powders after heat treatment at 900 °C for 2 h present single phase of HAP. (Fig. 2.) shows the X-ray patterns of HAP at 900 °C. The X-ray patterns of HAP using PEG 1000 at 900 °C are shown in (Fig. 3).

These patterns are in good agreement with the ASTM data (JCPDS) file (no. 09-0432) for hydroxyapatite. No characteristic peaks of impurities, such as calcium hydroxide and calcium phosphates were observed, meaning that

phase pure HAP was prepared under the present experimental conditions. The diffraction peaks particularly in the planes (0 0 2), (2 1 1), (1 1 2) and (3 0 0) are high and narrow implying that the HAP crystallizes well.

Fig. 1. Preparation of nanoparticles of HAp / PEG 1000

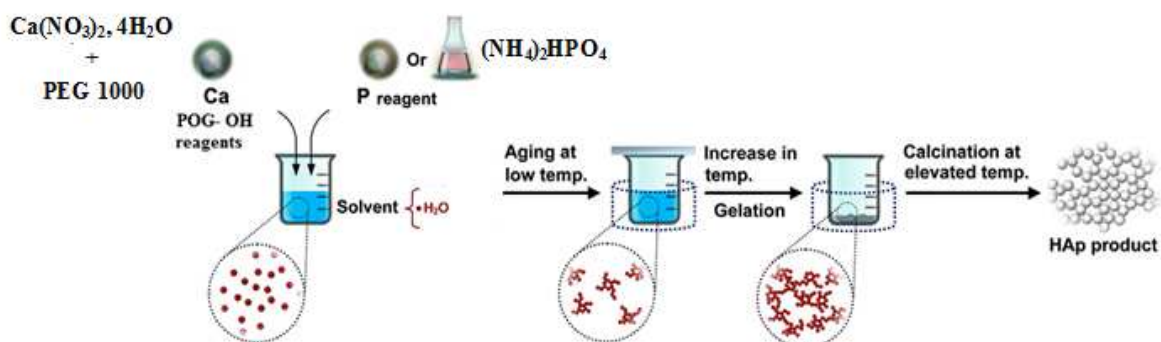


Fig. 2. XRD pattern of HAp calcined at 900 °C

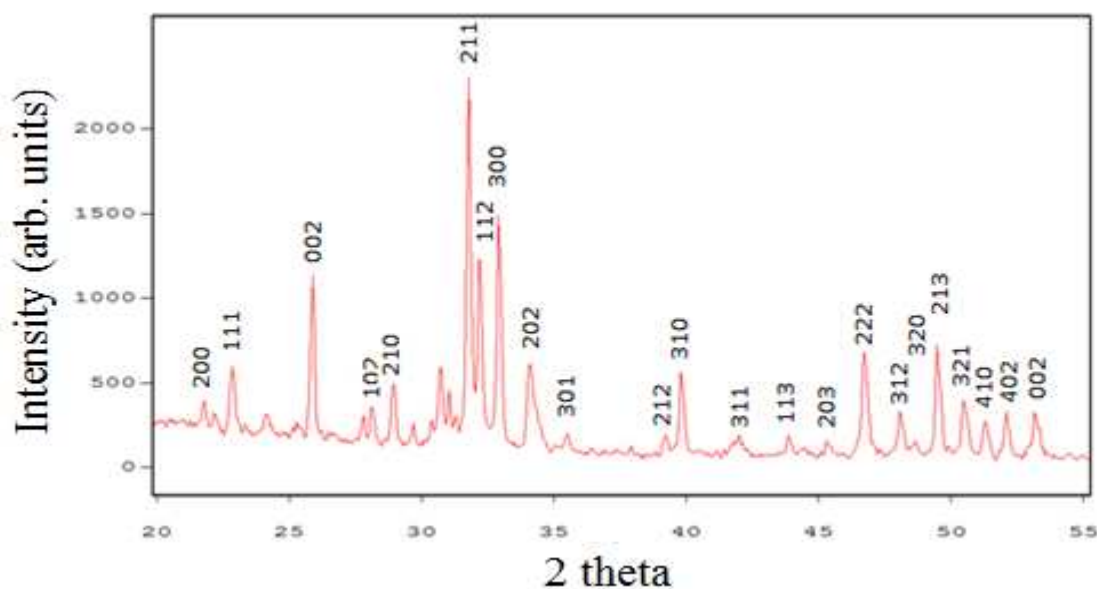


Fig. 3. XRD pattern of HAP using PEG 1000 calcined at 900 °C

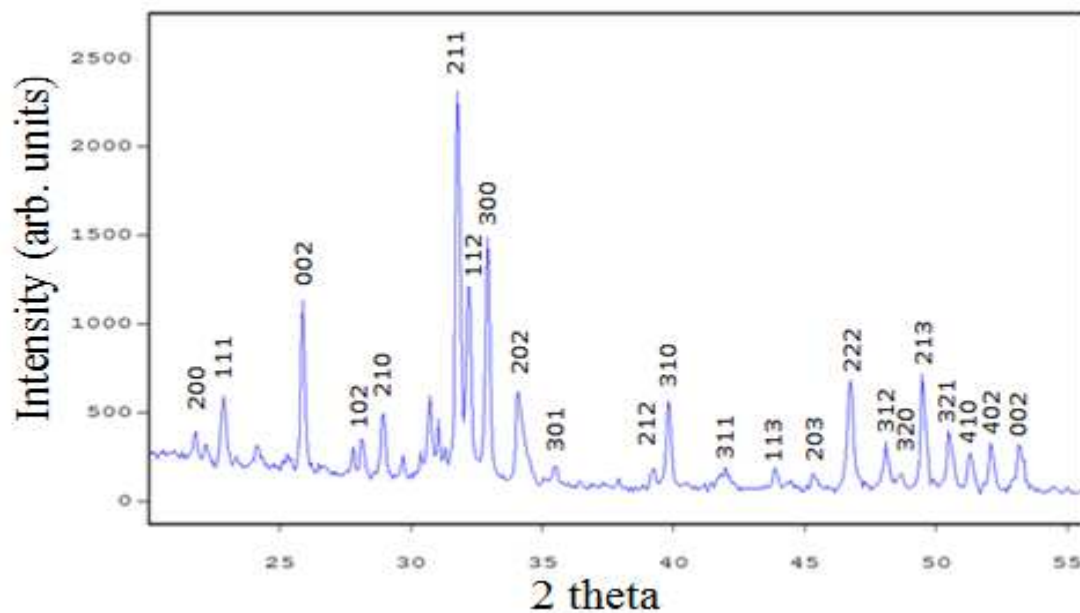


Fig.4. FTIR spectra of the (A) pure hydroxyapatite and (B) hydroxyapatite using polyethylene glycol 1000

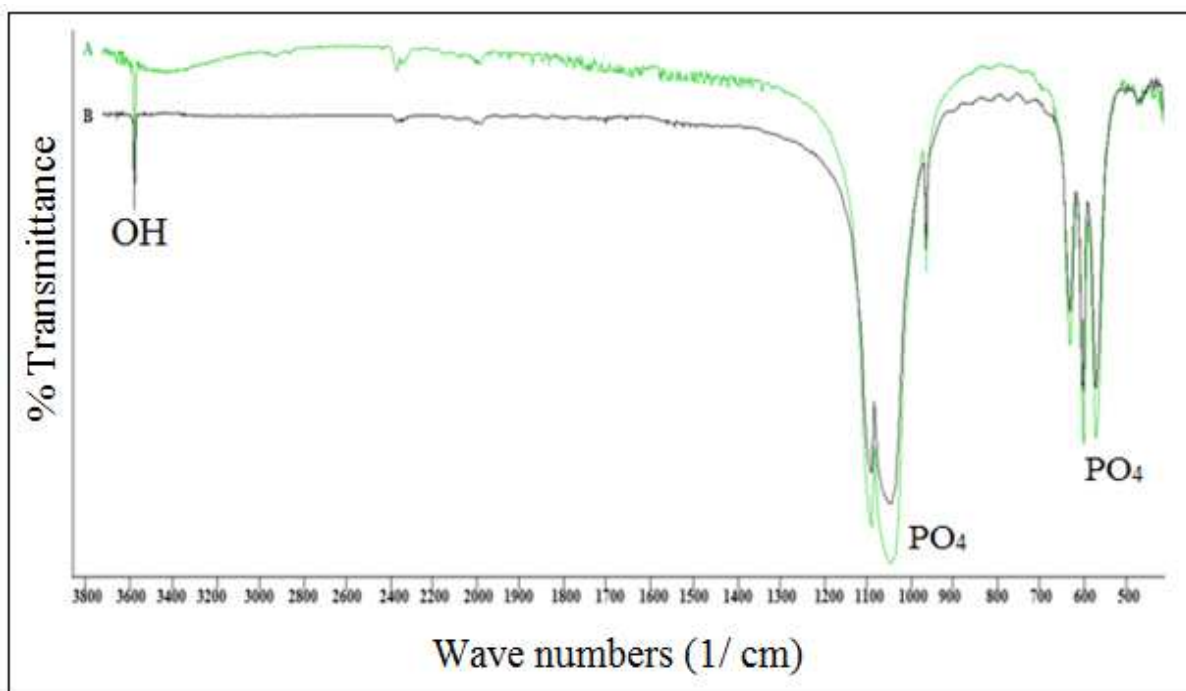
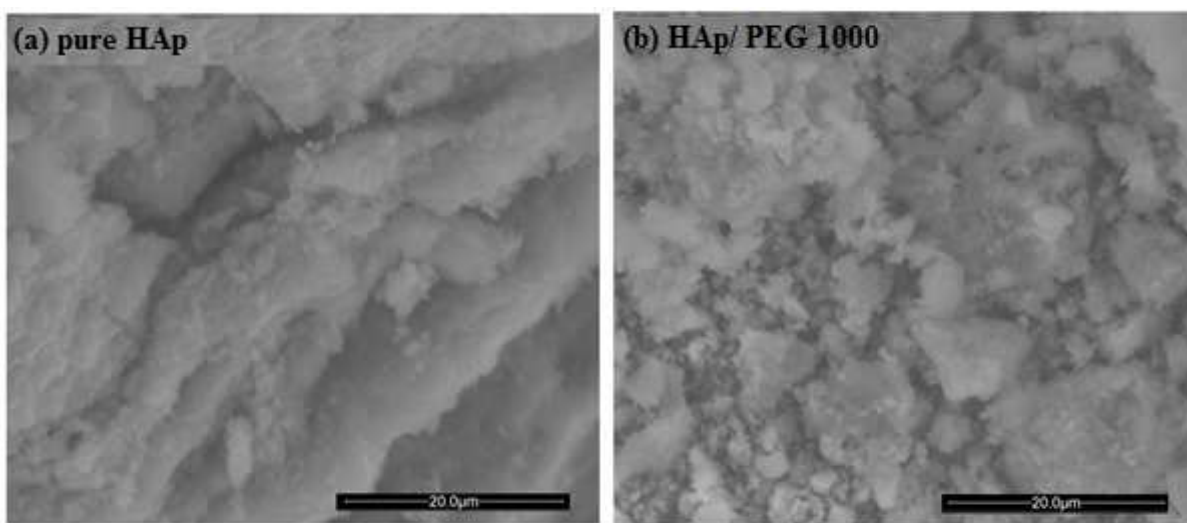


Fig. 5. SEM micrographs of HAP using polyethylene glycol at 85 °C



### 3.1.2. FTIR analysis

The FTIR spectra of the washed HAP and HAP using polyethylene glycol 1000 as modifier are shown in (Fig. 4.).

The bands at 3572 and 632  $\text{cm}^{-1}$  belong to the vibration of hydroxyl (O–H) group, the bands at 1089, 1045 and 962  $\text{cm}^{-1}$  are the characterization of phosphate stretching vibration and the bands observed at 601, 570  $\text{cm}^{-1}$  are due to the phosphate being in vibration. From the IR analysis, the precipitated powders are proved to be hydroxyapatite in nature. The presence of polyethylene glycol in hydroxyapatite does not play any role in the structural deformation of hydroxyapatite, meaning that HAP crystallites were prepared.

### 3.1.3. Morphology and particle size

The Fig. 5 shows the SEM micrographs of HAP using polyethylene glycol as modified. The small particles are seen agglomerated with an average diameter of 50–60 nm. The figure shows also pores, these pores are beneficial for the circulation of the physiological fluid throughout the coatings when it is used as a biomaterial in bone implantation. The pure HAP sintered at 900 °C for 2 h in stagnant air exhibits the morphology of clusters of grains structure as shown in Fig. 6(a). In Fig. 6 (b), the powder modifier by PEG 1000 obtained after heat treatment at 900 °C for 2 h, of the morphology of agglomerated grains.

Fig. 6. (a) SEM micrographs of HAp using polyethylene glycol 1000 at 900 °C and (b) SEM micrographs of pure HAp at 900 °C

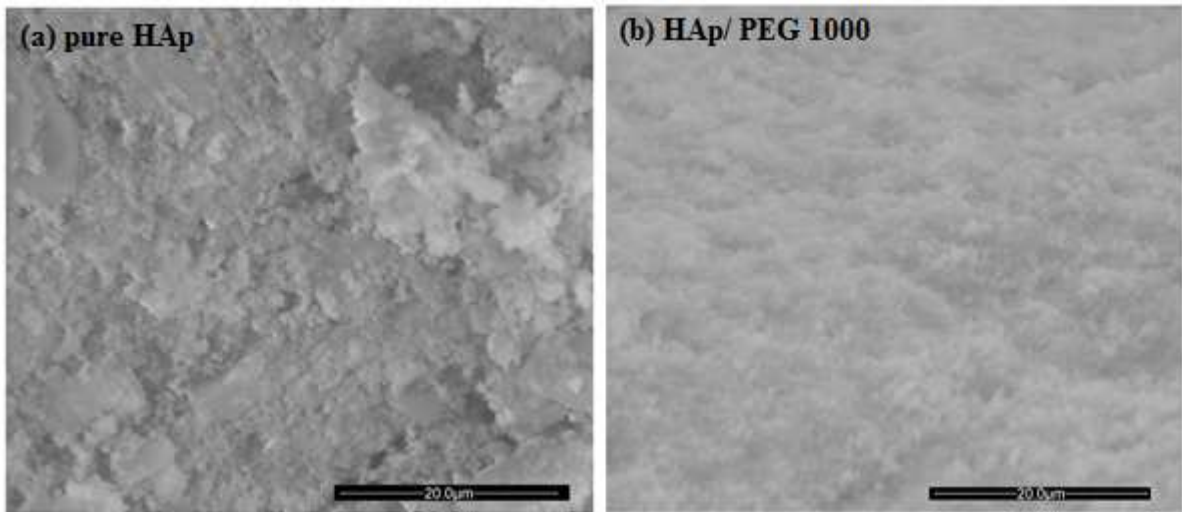


Fig. 7. EDAX spectrum of HAp/ PEG 1000

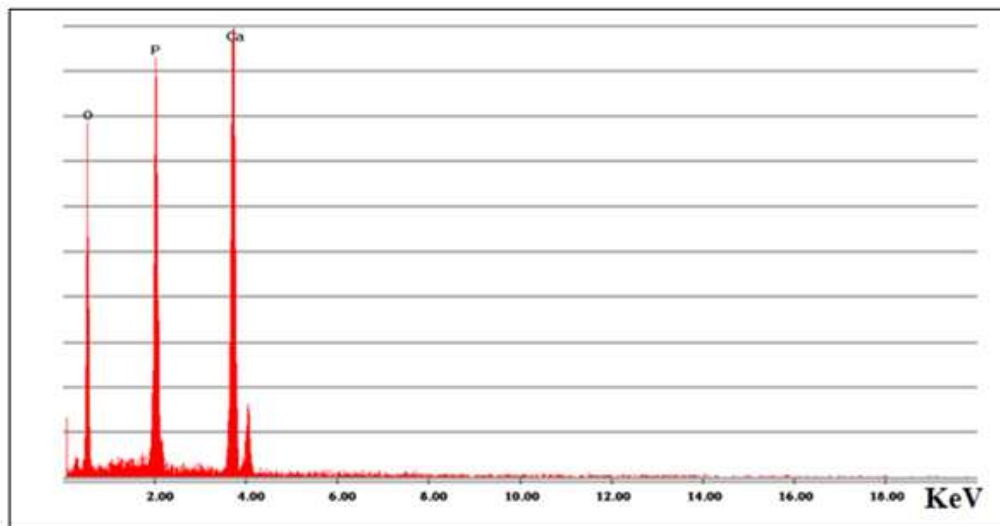


Fig. 8. Swelling ratio of HAp and HAp/ PEG 1000

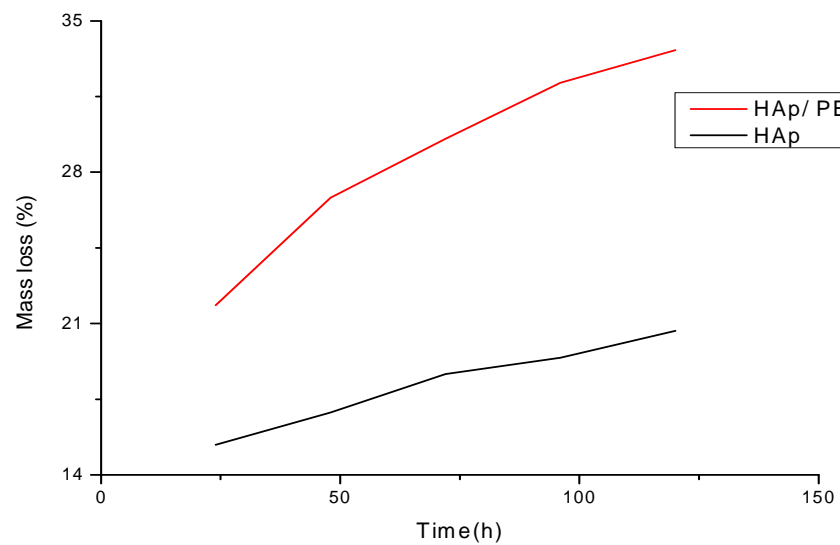


Fig. 9. The stereochemical structure of PEG 1000 and schematic illustration of the possible process of the forming of Hap

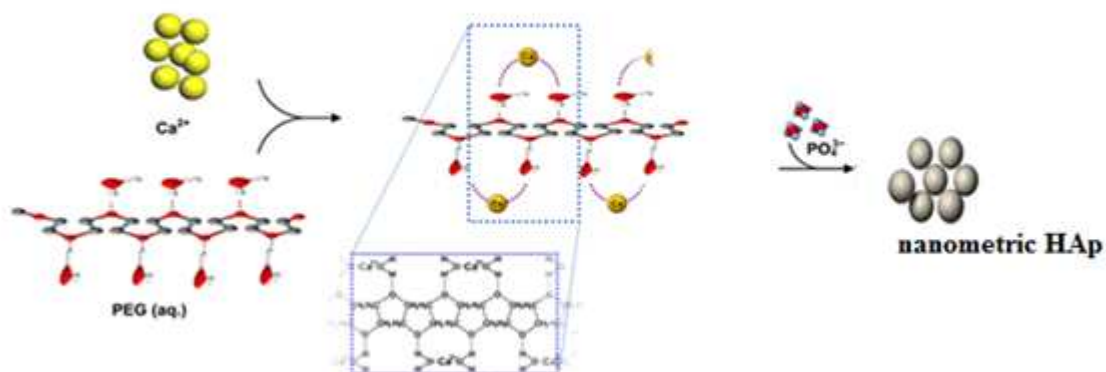


Fig. 10. Chromatogram of BPA desorbed from (A) hydroxyapatite using polyethylene glycol 1000 at 85 °C and (B) pure hydroxyapatite at 85 °C

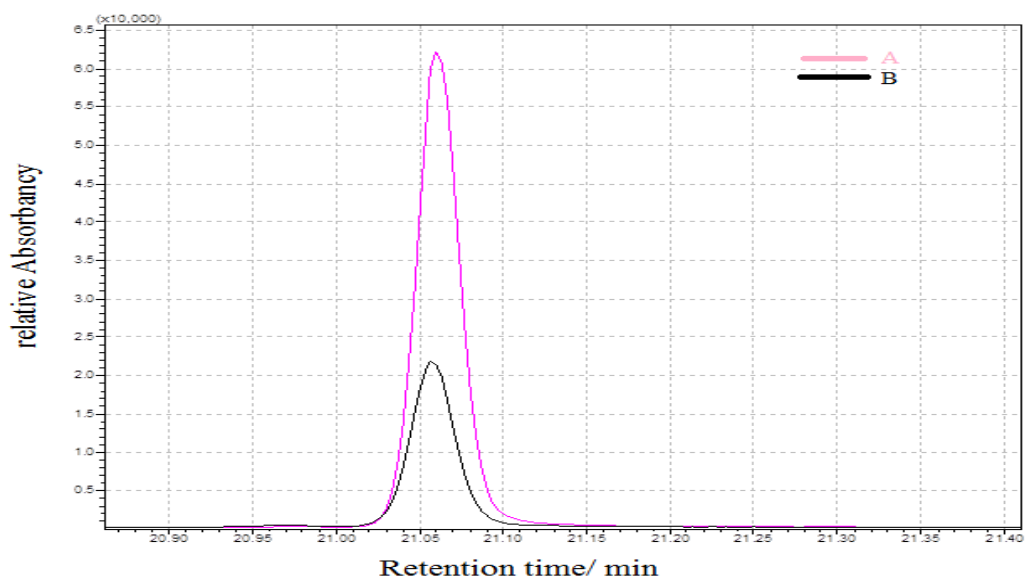


Fig. 11. Chromatogram of BPA desorbed from (A) hydroxyapatite using polyethylene glycol 1000 sintered at 900 °C and (B) pure hydroxyapatite calcined at 900 °C

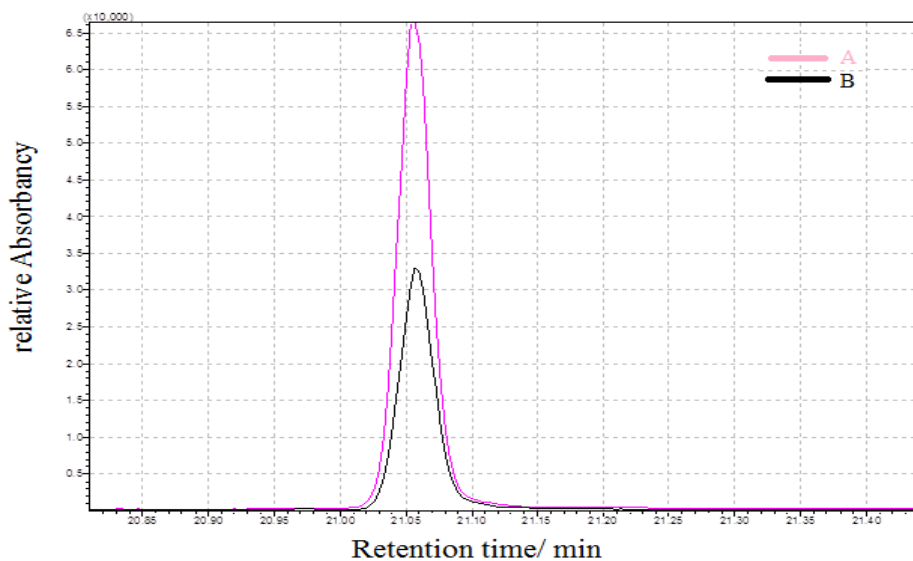
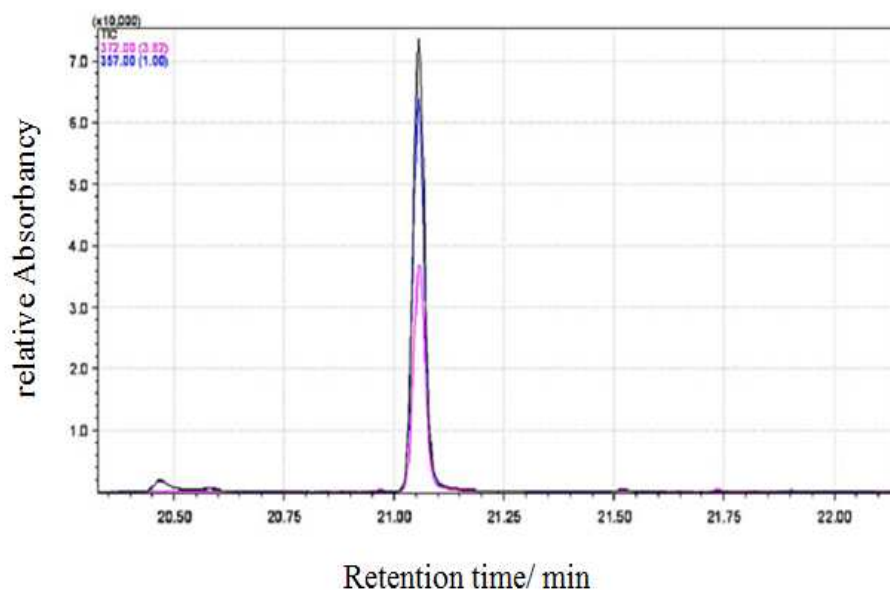


Fig. 12. Chromatogram of BPA desorbed from commercial florasil



The elemental analysis (EDAX) of HAp and HAp/ PEG 1000 can demonstrate similar composition as shown in Fig. 7. Mineral composition (calcium phosphate: Ca, O and P).

#### 3.1.4. Comparative study of swelling of composite HAp / PEG 1000 and pure HAp

The Fig. 8 shows the swelling kinetics during a 24 hour period, and the swelling of the HAp and composite HAp/ PEG 1000.

- The HAp pure present inflation rate of 19,41 %.
  - The composite of the HAp/ PEG 1000 a swelling ratio 28,23 %.
- This is explained by the presence of polymers that are responsible for the swelling phenomenon.

## DISCUSSION

The stereochemistry structure of PEG in the absence of water or in the aqueous solution and the possible formation process of HAp in the presence of PEG 1000 are shown in Fig. 9.

When PEG 1000 was dissolved in the aqueous solution, the PEG–OH bond was formed [18]. PEG molecule has the ability to chelate  $\text{Ca}^{2+}$  [20], therefore, PEG–OH can attract  $\text{Ca}^{2+}$  released from the  $\text{Ca}(\text{NO}_3)_2 \cdot 4\text{H}_2\text{O}$  to form the bond of PEG–O– $\text{Ca}^{2+}$ –O–PEG, then PEG–O– $\text{Ca}^{2+}$ –O–PEG reacted with the  $\text{PO}_4^{3-}$  released from  $(\text{NH}_4)_2\text{HPO}_4$  to produce HA crystal nucleus. In this process, the release rate of  $\text{Ca}^{2+}$  and  $\text{PO}_4^{3-}$  are the important factor. Experiments show that a large amount of deposits form in a short time when the solution was in the absence of PEG or the concentration of PEG was quite low, indicating HAp produced quickly. With increasing the concentration of PEG, initial deposits were gradually reduced and it required longer time to produce large quantities of deposits, indicating that PEG reduced the release rate of  $\text{Ca}^{2+}$  and restrained the formation of HAp crystal nucleus. When the release rate of  $\text{Ca}^{2+}$  and the deposit rate of HAp crystal nucleus deposited in the precipitation center achieved a dynamical equilibrium, HAp crystal nucleus deposited isotropically, and finally the spherical HAp particles were obtained. When the concentration of PEG 1000 was low, the release rate of  $\text{Ca}^{2+}$  were very fast and a large number of HAp crystal nucleus were produced, HAp crystal nucleus could not deposited isotropically in the precipitation center, so the morphology of as-prepared HAp particles were not spherical.

### 3.3. Chromatogram of BPA desorbed from the powders HAp modified by PEG 1000

The powders modified by PEG 1000 and pure HAp were tested and compared with florasil (60-100 mesh). All thin powders extractions were examined using BPA standard in water as the testing substance. The obtained data (Fig.10- 11) were compared with those for commercial florasil (Fig. 12.).

Various extraction times of TFME-BPA extraction were taken into consideration but the time 15 min (under stirring and sonication) was sufficient for reproducible results.

The comparison of extraction determined by extraction mass of BPA for the tested thin powders and florisil shows the efficiency of extraction for BPA after extraction of standard solution S2 with various thin powders. The most efficient extraction was obtained by HAp/PEG (adsorption on the thin powder modified by PEG 1000). On the other hand low retention rate were obtained by pure HAp. Another interesting result is that higher sorption level was observed in the powder modify by PEG 1000 sintered at 900 °C (PEG 1000 modified nanometric crystal surface).

### CONCLUSION

Nanomaterials are greatly promising in the development of more valuable orthopaedic and dental implants. In the present work, a novel HAp/ PEG 1000 nanocomposites was prepared by simple chemical route. The composition of PEG 1000 shows significant influence on particle size, the size of Hap particles decrease with increase in PEG concentration in the composite. Another interesting result is that the high level of sorption was observed in the powder modified by PEG 1000 compared to that of HAp only. However, the mechanism of interaction between HAp/ PEG 1000 and biologic systems should thoroughly be investigated and applied in vitro, in vivo processes to validate its use for medical applications.

### REFERENCES

- [1] A Ruban Kumar, S Kalainathan *Physica B* (2010), 405, 2799–2802
- [2] T Kokubo, HM Kim, M Kawashita, *Biomaterials* (2003), 24, 2161
- [3] K Chang, W Weng, G Han, P Du, G Shen, J Wang, JMF Ferreira, *Mater Res Bull* (2003), 38, 89
- [4] K Cheng, G Shen, W Weng, G Han, JMF Ferreira, J Yang, *Mater Lett* (2001), 51, 37
- [5] HS Liu, TS Chin, LS Lai, SY Chiu, KH Chung, CS Chang, MT Lui, *Ceram Int* (1997), 23, 91
- [6] M Toriyama, A ravaglioli, A Krajewski, G Gelotti, A Piancastelli, *J Eur Ceram Soc* (1996), 16, 429
- [7] M Otsuka, Y Matsuda, J Hsu, J Fox, W Higuchi, *Bio-Med Mater Eng* (1994), 4, 357
- [8] Y Liu, W Wang, Y Zhan, C Zheng, G Wang, *Mater Lett* (2002), 56, 496
- [9] A Milev, GSK Kannangara, B Ben-Nissan, *Mater Lett* (2003), 57, 1960
- [10] Y Han, S Li, X Wang, X Chen, *Mater Res Bull* (2004), 39, 25
- [11] G Guo, Y Sun, Z Wang, H Guo, *Ceram Int* (2005), 31, 869
- [12] L Yan, Y Li, ZX Deng, J Zhuang, X Sun, *Int J Inorg Mater* (2001), 3, 633
- [13] Y Han, S Li, X Wang, X Chen, *Mater Res Bull* (2004), 39, 25
- [14] J Liu, K Li, H Wang, M Zhu, H Yan, *Chem Phys Lett* (2004), 396, 429
- [15] K Azzaoui, M Berrabah, E Mejdoubi, A Lamhamdi, A Elidrissi, B Hammouti, *A Res Chem Intermed* DOI 10.1007/s 11164-1115-2 (2013)